

Synthesis and Characterization of Guanidine derivatives of Benzothiazole and their Cobalt(II), Nickel(II), Zinc(II), Copper(II) and Iron(II) Complexes.

Aremu, J. A., Durosinmi, L. M., Oluyemi, E.A. and Ojo, I.A.O.

Department of Chemistry, Obafemi Awolowo University, Ile-Ife, Nigeria

*Corresponding Author: **Durosinmi, L.M.**

Abstract: Guanidine and phosphonate derivatives of Benzothiazole, guanidinobenzothiazole, (GBT), guanidinophosphonatebenzothiazole, (GPBT) were synthesized along with their metal complexes, Fe(II), Co(II), Ni(II) Cu(II) and Zn(II). They were characterized by ^1H NMR, ^{13}C NMR, C.H.N analysis, percentage metal composition, FT-Infrared spectra analysis, UV-Visible electronic spectroscopy and magnetic susceptibility measurements.

The results from the percentage composition of the metals in the complexes suggest that ratio of the metal to ligands is 1: 2 (M: L) where M = Fe(II), Co(II), Ni(II), Cu(II) and Zn(II). Thus, the prepared complexes have the general formulae $[\text{ML}_2]$.

Spectral analyses revealed that the nitrogen in the imidazolic, exocyclic and the terminal end of the ligands are the coordination sites. The electronic spectral data and the values of the magnetic moments suggest octahedral geometry for all the complexes except copper(II) complexes with a distorted octahedral geometry.

Keywords: Characterization, guanidine derivatives, metal complexes, synthesis.

Date of Submission: 11-01-2018

Date of acceptance: 25-01-2018

I. Introduction

Guanidine derivatives constitute a very important class of therapeutic agents suitable for treatment of a wide spectrum of diseases, [1]. Guanidine and phosphonate compounds have wide area of interesting biochemical and pharmaceutical properties [2] and heterocyclic compounds containing hetero atoms such as Nitrogen, oxygen and sulphur are essential to life in various ways [3].

Thus, guanidines, phosphonates and their complexes continue to receive attention both in academic research and industrial development as compounds with unique properties, [4]. Furthermore, investigations on the complexing ability of metal ions with ligands assist in understanding the function of physiological systems due to their industrial and biological applications, [5]. Phosphonates are highly water-soluble and poorly soluble in organic solvents. Despite their ubiquitous uses as pharmacological agents, synthesis of phosphonates still remains a formidable challenge, [6], [7]. Generally, preparation of guanidine derivatives *via* primary amines is carried out using thiourea bearing one or more electron-withdrawing groups in the presence of mercury(II) or copper(II) salts and a base, [8].

Thus, thioureas are common reagents for synthesis of guanidines. Their conversion into guanidine usually requires initial activation [2]. However, characterization, isolation or definition of active intermediates is not described in many cases. The guanidino and phosphonate derivatives were synthesized according to the methods of Alan and Boris, [2] and Krishnamurthy and Natarajan, [9]. Thiourea is converted into guanidines in tetrahydrofuran in the presence of tertiary amines.

II. Experimental

2.1. Reagents and Instrumentation

High grade analytical chemicals and reagents were used. 2-amino benzothiazole, silica gel, copper (II) sulphate, thiourea, tetrahydrofuran, triethylamine, dimethylphosphite, perchloric acid, disodium ethylene diamine tetra acetic acid (EDTA), zinc (II) sulphate, ammonia solution, ammonium chloride, erichrome black T indicator, sodium hydroxide, methyl thymol blue indicator, Iron (II) chloride, cobalt (II) nitrate, nickel (II) nitrate, copper (II) nitrate, zinc (II) nitrate, purchased from Sigma Aldrich.

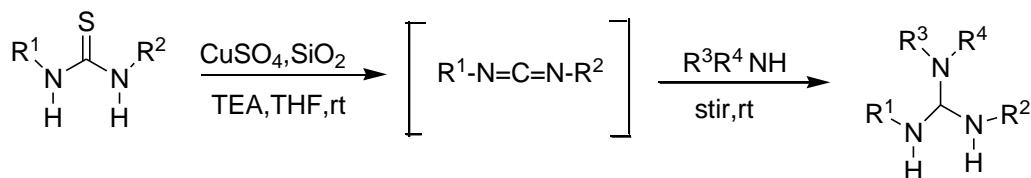
The NMR spectra were recorded on Agilent-NMR-400 MHz Spectrometer; IR spectra ($4000-400\text{ cm}^{-1}$) were recorded on Shimadzu FTIR- 8700 Spectrophotometer. The C.H.N elemental analyses were carried out on Perkin Elmer 240 C elemental analyzer and the electronic transitions using the UV Visible Spectrophotometer.

Column chromatography analysis was carried out for purification of the crude guanidinophosphonatebenzothiazole ligand. Melting points of the samples were determined by using the Electro

thermal Digital Melting Point Apparatus. The magnetic susceptibility measurements of the metal complexes were made at room temperature using MSB-MK1 Sherwood Susceptibility Balance.

2.2. Synthetic Methods: Guanidination and Phosphorylation of Benzothiazole.

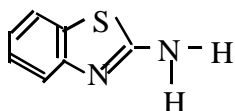
Thioureas are converted into guanidines using a suitable solvent such as tetrahydrofuran and chloroform containing copper sulphate – silica gel in presence of tertiary amines, [2]. The procedure allows preparation of a very wide range of substituted guanidines. Electron withdrawing substituents in the thiourea fragment accelerate the reaction.



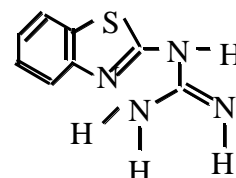
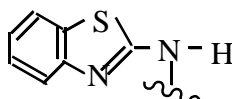
$\text{R}^1, \text{R}^2, \text{R}^3, \text{R}^4 = \text{Alkyl or Aryl}.$

Traditionally, organophosphonates are prepared via a Michaelis-Arbuzov or a Michaelis-Becker reaction utilizing the nucleophilic properties of trivalent phosphorus compounds (e.g. trialkylphosphites or alkali metal salts of dialkyl phosphates) in the presence of alkyl halides, [10]. Depending on the methods of choice, these conventional reaction conditions often are not convenient, requiring elevated temperature, the use of a strong anhydrous base, and very long reaction times. Moreover, these procedures often lead to a complicated mixture of side products or result in poor yields of the phosphonate. Therefore, to circumvent these problems, more methods are being embarked upon for improved procedure or the synthesis of the phosphonates.

Guanidinobenzothiazole and guanidinophosphonatebenzothiazole were synthesized according to the methods of Alan and Krishnamurthy, [2,9].



2 – Aminobenzothiazole



Guanidinobenzothiazole.

2.3. Syntheses of Guanidinobenzothiazole, (GBT).

Copper (II) sulphate and silica gel (1 g each) were added to 25 ml of tetrahydrofuran in the presence of 2 ml triethylamine in a 250 ml round bottom flask. Thiourea, 3.81 g (50 mM) was added and the solution was stirred at room temperature for 6 Hr. to produce carbondiamide intermediate. The intermediate was reacted with 2-Aminobenzothiazole by stirring again for 6 hr at room temperature. It was filtered and the filtrate was concentrated by using rotary evaporator. The crystal was washed with few mls of tetrahydrofuran and dried. The yield, melting point and other analytical data are presented in Table 1.

2.4. Synthesis of Guanidinophosphonatebenzothiazole, (GPBT).

Excess paraformaldehyde, guanidinobenzothiazole (5 mM, 0.96 g) and 60 mg of silica-supported perchloric acid were stirred for 8 hr in 25 ml of ethanol. Dimethylphosphite (50 mM, 4.50 ml) was then added and the stirring continued for 1 hr at room temperature. It was transferred into an oil bath and refluxed at 80 °C with stirring for 8 hr. The cooled solution mixed with 100 ml of dichloromethane was washed with 100 ml of deionized distilled water in a separating funnel and dried with anhydrous sodium sulphate for 24 hr and then filtered. The filtrate was concentrated by using rotary evaporator. The crude guanidinophosphonatebenzothiazole was purified using column chromatography. The yield, melting point and other analytical data are presented in Table 1.

2.5. Synthesis of metal complexes of Guanidinobenzothiazole and Guanidinophosphonatebenzothiazole.

The syntheses were carried out according to the method of Anitha *et al.*, [11] and Bakiret *et al.*, [12]. Equimolar quantities (0.5 mM) of the ligand and metal (II) salt were reacted in 25 ml of ethanol in a 250 ml round bottom flask (where ligand = guanidinobenzothiazole, metal (II) salt = cobalt (II) nitrate, nickel (II) nitrate, copper (II) nitrate and zinc (II) nitrate). The solution was stirred at room temperature for 18 hr. It was immediately followed by 4 hr reflux at 80 °C in an oil bath. The solution was cooled, filtered and concentrated by using rotary evaporator. The crystal was washed with ethanol and dried in a desiccator over activated silica gel. The colours, yields, melting points and other analytical data are presented in Table 1.

2.6. Characterization of the ligands and complexes

The ligands and the complexes were characterized by spectrometry analysis for structural elucidations using Agilent NMR-400 MHz, FT-IR-8700 SHIMADZU Fourier Transform Infrared Spectrophotometer in the 4000–400 cm⁻¹ region, Sherwood Magnetic susceptibility balance, UV–Visible electronic spectrophotometer and Perkin Elmer 240C elemental analyzer for percentage composition of C, H, and N of the ligands. The ¹H-NMR of the ligands was recorded in DCOD solution.

2.7. Column chromatography

Column chromatography analysis was carried out for purification of the crude guanidinophosphonatebenzothiazole ligand. The column was packed in a burette. This was followed by the addition of treated sea sand as a bed for the column. N-hexane was added and this was followed by the addition of silica-gel. Little quantity of sea sand was added to the top of the silica-gel. A prepared paste of the sample was added to the top of the column. The column was not allowed to dry by refilling the burette in order to prevent the column from cracking. The eluent was received in a sample bottle wrapped with aluminum foil and the solvent was evaporated. Purity of the sample was determined by thin layer chromatography.

2.8. Complexometric titration of metal (ion) complexes of guanidinobenzothiazole (GBT) and guanidinophosphonatebenzothiazole, (GPBT),

The metal- guanidinobenzothiazole complex (GBT)/ guanidinophosphonatebenzothiazole, (GPBT), (0.05mM,) was mixed with 5 ml of concentrated nitric acid. The mixture was heated and evaporated to almost dryness on a hot plate. It was allowed to cool. Addition of little quantity of deionized distilled water was carried out three times and heated to almost dryness. It was allowed to cool and 10 ml of deionized distilled water was added. The solution was properly rinsed and transferred into a 50 ml standard volumetric flask and made up to mark.

10 ml of the complex solution was pipetted into a 250 ml conical flask followed by addition of 4 ml of 1M sodium hydroxide solution. Methyl thymol blue indicator was added and the solution was titrated with standardized EDTA in three replicates and average titre was calculated. At the end point, the colour changed from blue to grey. This procedure was repeated for all the complexes. Percentage metal composition in each of the complexes was therefore determined.

2.9. Percentage composition of metals in the complexes.

This analysis was carried out by complexometric titration through titration of the digested complex with standardized disodium salt of ethylenediaminetetraacetic acid. The molarity of the EDTA obtained when standardized with 0.01 M (1.61 g) of Zinc salt multiplied by the volume of EDTA obtained when titrated with the digested complex multiplied by the molar mass of the metal multiplied by 100 divided by the volume (10 ml) of the complex solution divided by 20 since the solution of the complex was prepared in 50 ml standard volumetric flask divided by the mass of the complex digested.

III. Results And Discussion

3.1. Analytical data of Guanidinobenzothiazole and guanidinophosphonatebenzothiazole and the metal complexes.

The analytical data such as colours, percentage yields and the melting points of the ligands guanidinobenzothiazole, (GBT), guanidinophosphonatebenzothiazole, (GPBT) and their complexes are presented in (Table 1). The complexes exhibited different shades of colours, characteristic of transition metal complexes, [11].

3.2. C,H, N Analysis

The CHN elemental Analysis of GBT and presented in Table: 2

3.3. Percentage composition of the metals in the complexes

The results from calculations and the inferences from the percentage composition of the metals in the complexes suggest that ratio of the metal to ligands is 1 : 2 (M : L) where M = Fe(III), Co(II), Ni(II), Cu(II) and Zn(II) and L for guanidinobenzothiazole and guanidinophosphonatebenzothiazole. The prepared complexes were therefore found to have the general formulae $[ML_2]$.

3.4. 1H NMR Spectra of guanidinobenzothiazole (GBT), guanidinophosphonatebenzothiazole, (GPBT).

1H NMR spectra of GBT, GPBT were recorded on an Agilent-NMR 400 NMR-400MHZ. TMS was used as the internal standard. In the 1H -NMR spectra of the guanidinobenzothiazole ligand (Figure 5), the aromatic protons of the benzene ring resonated at a chemical shift of 6.80 to 7.60 ppm while that of the exocyclic NH proton was observed at 3.20 to 3.60 ppm and the terminal NH_2 with $C=NH$ moiety was seen as a singlet at chemical shift around 1.00-1.20 ppm, [13].

1H -NMR spectrum of the guanidinophosphonatebenzothiazole, (Figure 6) indicated the characteristic integration pattern of the benzene aromatic ring proton around 7.00-7.90 ppm. The chemical shift, δ , assigned to the resonance due to the exocyclic hydrazino N-H in the proton spectrum of the free guanidinophosphonatebenzothiazole ligand was observed around 4.20-6.30 ppm with a reflection of mesomeric effect. The peak for the N-H with $C=NH$ proton was observed around 1.00 ppm. The δ 2.40-2.80 ppm appeared as an evidence of P-C-H present in the guanidinophosphonatebenzothiazole ligand, [14]. The signal in the region 3.00 – 4.00 ppm is ascribed to the resonance due to the presence of $PO(OCH_3)_2$ as equivalent protons due to their presence in the same environment. The chemical shift results support the proposed structure of the ligands, Figures 1 and 2.

The chemical shift assignments are summarized in Table 4. The assignments are similar to the literature values, [14].

3.5. ^{13}C NMR spectra of guanidinobenzothiazole (GBT), guanidinophosphonatebenzothiazole, (GPBT).

In the ^{13}C -NMR spectrum of the guanidinobenzothiazole ligand (Figure 7), the chemical shift ascribed to the resonance due to the position 2 carbon of the imidazolic ligand appeared at 186 ppm which could be attributed to the presence of the sulphur atom in the system, [15]. The signal at 167 ppm is due to the aliphatic C_{11} . The value indicates the deshielding effect, [15]. The chemical shifts assigned to the resonance due to carbons of the benzene aromatic ring of this ligand were observed at different chemical shifts based on their different chemical environments as 152 ppm for carbon 9, 131 ppm for carbon 6, 125 ppm for carbon 5, 121 ppm for carbon 8, 120 ppm for carbon 7 and 117 ppm for carbon 4, [15].

The ^{13}C NMR spectrum at 169 ppm assigned to the resonance due to the carbon at position 2 for the imidazolic carbon and 138 ppm for the carbon at position 11 supported the proton NMR spectra results for the structure proposed for guanidinophosphonatebenzothiazole, (Figure 2). The characteristic integration pattern of the aromatic moieties at C_9 with chemical shifts of 127 ppm, 126 ppm for C_6 , 123 ppm for C_5 , 118 ppm for C_8 , 97 ppm for C_7 and 95 ppm for C_4 were also in agreement with the results of the proton NMR. The signals at 64 ppm and 48 ppm were observed as a consequence of resonance ascribed to carbons 16 and 17 of $PO(OCH_3)_2$ and carbon 14 of the methyl group in the guanidinophosphonatebenzothiazole ligand, [14].

3.6. FT-Infrared Spectra of the Ligands and the Complexes .

The infra- red spectrum of the guanidinobenzothiazole ligand, (Figure 9), shows absorption peaks in the region 3394 cm^{-1} - 3271 cm^{-1} due to the $\nu(N-H)$ stretching vibration of the amine groups. The peak at 1450 cm^{-1} can be ascribed to $\nu(C=N)$ stretching vibration while the strong absorption band at 1103 cm^{-1} is characteristic of the $\nu(C-N)$ vibration. The stretching vibration of aromatic $\nu(C-H)$ occurs at about 3093 cm^{-1} while the absorption band at 1635 cm^{-1} indicates the presence of aromatic $\nu(C=C)$ stretching frequency vibration of the guanidinobenzothiazole ligand.

The broadness in the region, 3394 cm^{-1} - 3271 cm^{-1} as well as the shifts of the band to lower values in the metal-GBT complexes suggest coordination of the metal ions to the guanidinobenzothiazole through the nitrogen atoms, [16, 11].

The new positions are 3155 cm^{-1} for Fe(III)-GBT, 3371 cm^{-1} for the Co(II) –GBT, 3371 cm^{-1} for the Ni(II)-GBT and 3201 cm^{-1} for Zn(II)-GBT. For Cu(II)-GBT, there is a broad band at 3409 cm^{-1} (Figures 10-14).

In the complexes, the bands due to the aromatic $\nu(C-H)$ and $\nu(C=C)$ stretching frequency vibrations remained almost constant suggesting the non-involvement of the aromatic proton $\nu(C-H)$ and the $\nu(C=C)$ in the complex formation. This is not unexpected.

However, the $\nu(C-N)$ vibration band at 1103 cm^{-1} in the spectrum of guanidinobenzothiazole shifted to lower frequencies in the metal –GBT complexes; 1002 cm^{-1} for Fe(III)-GBT, 1041 cm^{-1} for Co(II)-GBT, 1010 cm^{-1} for Cu(II)-GBT and 1026 cm^{-1} Zn(II)-GBT indicating coordination of the nitrogen to the metal ions, [17, 18]. The frequency for the Ni(II)-GBT complex was however higher, 1118 cm^{-1} .

The band at 1450 cm^{-1} in the GBT due to $\nu(\text{C}=\text{N})$ shifted to 1380 cm^{-1} , 1396 cm^{-1} , and 1388 cm^{-1} for Co(II)-GBT, Ni(II)-GBT and Cu(II)-GBT.

Asymmetric and symmetric $\nu(\text{C}-\text{S})$ stretching vibrations are assigned to the weak bands in the region $740\text{--}632\text{ cm}^{-1}$, [19]. The bands remained almost constant in the metal complexes. This indicates the non-involvement of the sulphur atom in the coordination to the metal ions.

IR spectra peaks at 501 cm^{-1} for Fe(II), 493 cm^{-1} for Co(II) and Ni(II), 424 cm^{-1} for Cu(II) and 555 cm^{-1} for Zn(II) are evidences for the $\nu(\text{M}-\text{N})$ absorption frequencies, [12].

3.6.1 Guanidinophosphonatebenzothiazole, GPBT

The $\nu(\text{N}-\text{H})$ stretching frequency of 3417 cm^{-1} in IR spectrum of the guanidinophosphonatebenzothiazole ligand (Figure 15) shifted to broad bands at 3163 cm^{-1} for Fe(II)-GPBT, 3394 cm^{-1} for Co(II)-GPBT, 3386 cm^{-1} for Ni(II)-GBT, 3348 cm^{-1} for Cu(II)-GPBT and 3224 cm^{-1} for Zn(II)-GPBT. The shifts in the position of the bands indicate the coordination of the ligand through the nitrogen atoms present in the hydrazino position of the ligand, [5].

Similarly, the band at 1442 cm^{-1} due to the $\nu(\text{C}=\text{N})$ in the free ligand moved to 1380 cm^{-1} in the Fe(III)-GPBT, 1388 cm^{-1} in Co(II)-GPBT, 1380 cm^{-1} for Ni(II)-GPBT, 1396 cm^{-1} and 1342 cm^{-1} for Cu(II)-GPBT and Zn(II)-GPBT, (Figures 16-20),

The peaks at 1172 cm^{-1} , 3263 cm^{-1} and 1635 cm^{-1} are attributed to stretching frequency vibration bands of $\nu(\text{C}-\text{N})$, aromatic $\nu(\text{C}-\text{H})$ and aromatic $\nu(\text{C}=\text{C})$ respectively (Mehmet, 2001) while the peak at 1072 cm^{-1} is assigned to the $\nu(\text{P}=\text{O})$, [20].

In the metal-GPBT complexes, the band at 1172 cm^{-1} assigned to $\nu(\text{C}-\text{N})$ shifted to lower frequencies at 1064 cm^{-1} for Fe(II), Cu(II), 1056 cm^{-1} for Ni(II). This further indicates the involvement of the nitrogen atoms in the coordination to the metal ions, [17]. However, for Co(II)-GPBT and Zn(II)-GPBT, the values are 1072 cm^{-1} and 1080 cm^{-1} respectively.

The peaks at 416 cm^{-1} for Fe(II)-GPBT, 563 cm^{-1} for Co(II)-GPBT, 578 cm^{-1} for Ni(II)-GPBT, 540 cm^{-1} for Cu(II)-GPBT and 555 cm^{-1} for Zn(II)-GPBT are evidences for the $\nu(\text{M}-\text{N})$ absorption frequencies, [12, 5].

3.7. UV-Visible Electronic Spectral Bands and Magnetic susceptibility measurements of guanidinobenzothiazole (GBT), guanidinophosphonatebenzothiazole, (GPBT) and their Complexes

The electronic spectra and magnetic susceptibility data for the free ligands and the metal complexes of guanidinobenzothiazole (GBT), guanidinophosphonatebenzothiazole, (GPBT) are shown in Table 7. The band observed at 222 nm in the guanidinobenzothiazole ligand (Figure 21) has been attributed to the absorption arising from the $\pi \rightarrow \pi^*$ electronic transitions while the transition around 260 nm characterized the $n \rightarrow \pi^*$ resulting from the lone pair of electrons, [21,22].

The spectrum of the Fe(III)-GBT shows absorption peak at 320 nm (Figure 22) which can be linked to charge transfer. Evidence for an octahedral geometry of the complex is supported by the 2.09 B.M magnetic susceptibility value which falls within the range of values for probable octahedral geometry. The Co(II)-guanidinobenzothiazole complex, (Figure 23) gave a peak around 530 nm . This is most likely due to the transition, ${}^4\text{T}_{1g}(\text{F}) \rightarrow {}^4\text{T}_{2g}(\text{F})$. This, together with magnetic moment value of 1.80 B.M suggests an octahedral geometry, [5].

The Ni(II) complex, (Figure 24) gave bands at 680 nm and 720 nm . These are attributable to ${}^3\text{A}_{2g}(\text{F}) \rightarrow {}^3\text{T}_{1g}(\text{F})$ and ${}^3\text{A}_{2g}(\text{F}) \rightarrow {}^3\text{T}_{1g}(\text{P})$ transitions and they indicate octahedral geometry. This is further established by the magnetic moment value of 3.14 B.M (Table 7).

The Cu(II)-GBT complex gave a peak around 780 nm attributed to ${}^2\text{E}_g - {}^2\text{T}_{2g}$ transition suggesting distorted octahedral geometry, [12]. This agrees with the result of the magnetic susceptibility of 2.10 B.M which also falls within the range for probable octahedral geometry.

The Zn(II) guanidinobenzothiazole complex (Figure 26) exhibited transition due to charge transfer at 730 nm . The zero value of the magnetic susceptibility is not unexpected in view of its characteristic d^{10} electronic configuration which also suggests an octahedral geometry for the complex, [5].

3.7.1. Guanidinophosphonatebenzothiazole, GPBT

The bands due to the $\pi \rightarrow \pi^*$ and $n \rightarrow \pi^*$ electronic transitions were observed at $220, 259\text{ nm}$ and 285 nm due to the characteristic absorption spectra (Figure 27.) of the free guanidinophosphonatebenzothiazole, [21]. Fe(III) complex of GPBT, (Figure 28) gave absorption peak at the region less than 400 nm which can be related to charge transfer. The magnetic moment of 2.04 B.M is an indication of octahedral complex.

The Co(II) complex, (Figure 29) gave a peak at 520 nm attributed to ${}^4\text{A}_2(\text{F}) \rightarrow {}^4\text{T}_1(\text{P})$. Magnetic susceptibility value of 1.80 B.M suggests an octahedral geometry, [18].

The spectrum of Ni(II)-guanidinophosphonatebenzothiazole complex indicated a peak at 630 nm which can be related to ${}^3T_1(F) \rightarrow {}^3T_1(P)$. This together with 3.09 B.M magnetic moment value found are indicative of an octahedral geometry.

For the Cu(II) complex, the magnetic moment value of 2.12 B.M observed is within the conceivable range for distorted octahedral geometry, [16]. For the electronic spectrum of Zn(II) - guanidinophosphonatebenzothiazole complex, the observed zero B.M magnetic moment of the complex indicates the diamagnetic nature of the Zn(II)-GPBT complex.

Table 1: Analytical data of Guanidine derivatives and the metal Complexes

Compounds	Empirical formula	Molecular weight	Yield (%)	Melting point (°C)	Colour
GBT	C ₈ H ₉ N ₄ S	193.00	87	69 – 71	Green
Fe-Cplx	[Fe(C ₈ H ₉ N ₄ S) ₂]	441.85	79	121 – 123	Brown
Co-Cplx	[Co(C ₈ H ₉ N ₄ S) ₂]	444.93	68	143 – 145	Brown
Ni-Cplx	[Ni(C ₈ H ₉ N ₄ S) ₂]	444.71	72	189 – 191	Green
Cu-Cplx	[Cu(C ₈ H ₉ N ₄ S) ₂]	449.55	77	116 – 118	Green
Zn-Cplx	[Zn(C ₈ H ₉ N ₄ S) ₂]	451.38	75	119 – 121	Green
GPBT	C ₁₁ H ₁₅ N ₄ SPO ₃	314.30	86	68 – 70	Pink
Fe-Cplx	[Fe(C ₁₁ H ₁₅ N ₄ SPO ₃) ₂]	683.85	71	130 – 132	Wine
Co-Cplx	[Co(C ₁₁ H ₁₅ N ₄ SPO ₃) ₂]	686.93	61	75 – 77	Brown
Ni-Cplx	[Ni(C ₁₁ H ₁₅ N ₄ SPO ₃) ₂]	686.71	72	151 – 153	Green
Cu-Cplx	[Cu(C ₁₁ H ₁₅ N ₄ SPO ₃) ₂]	691.55	76	108 – 110	Brown
Zn-Cplx	[Zn(C ₁₁ H ₁₅ N ₄ SPO ₃) ₂]	693.38	78	113 – 115	Brown

Table 2: C, H, N elemental Analysis of GBT and GPBT

L	Analysis Calculated (Found)		
	% C	% H	% N
GBT(C ₈ H ₉ N ₄ S)	49.98 (49.93)	4.19 (4.13)	29.14 (29.12)
GPBT(C ₁₁ H ₁₅ N ₄ SPO ₃)	43.63 (43.56)	5.80 (5.72)	16.96 (16.90)

Table 3: Percentage of metal in the complexes, the stoichiometry and the Probable formulae.

Compounds	% Metal Found	(Calculated)	Stoichiometry	Probable Formula
M- GBT				
[Fe(C ₈ H ₉ N ₄ S) ₂]	12.68	(12.64)	1:2	Fe(L) ₂
[Co(C ₈ H ₉ N ₄ S) ₂]	13.30	(13.24)	1:2	Co(L) ₂
[Ni(C ₈ H ₉ N ₄ S) ₂]	13.24	(13.20)	1:2	Ni(L) ₂
[Cu(C ₈ H ₉ N ₄ S) ₂]	14.18	(14.13)	1:2	Cu(L) ₂
[Zn(C ₈ H ₉ N ₄ S) ₂]	14.53	(14.48)	1:2	Zn(L) ₂
M –GPBT				
[Fe(C ₁₁ H ₁₅ N ₄ SPO ₃) ₂]	8.16	(8.17)	1:2	Fe(L) ₂
[Co(C ₁₁ H ₁₅ N ₄ SPO ₃) ₂]	8.60	(8.58)	1:2	Co(L) ₂
[Ni(C ₁₁ H ₁₅ N ₄ SPO ₃) ₂]	8.53	(8.55)	1:2	Ni(L) ₂
[Cu(C ₁₁ H ₁₅ N ₄ SPO ₃) ₂]	9.18	(9.19)	1:2	Cu(L) ₂
[Zn(C ₁₁ H ₁₅ N ₄ SPO ₃) ₂]	9.42	(9.43)	1:2	Zn(L) ₂

Table 4: ¹H-NMR chemical shift (δ) of GBT and GPBT.

S/N	Ligands	CH aromatic protons (ppm)	NH protons imidazol (ppm)	N-H protons Exo (ppm)	NH ₂ , C=NH protons Exo (ppm)	NH, C=NH protons Exo (ppm)	P-C-H proton (ppm)	PO(OCH ₃) ₂ (ppm)
3	GBT	6.80-7.60	--	3.20-3.60	1.00-1.20		---	---
4	GPBT	7.00-7.90		4.20-6.30		1.00	2.40-2.80	3.00 – 4.00

Table 5: ¹³C-NMR chemical shift (δ) of GBM, GPBM, GBT, GPBT

Compounds	C ₂ (ppm)	C ₄ -C ₇ (ppm)	C ₅ -C ₆ (ppm)	C ₈ -C ₉ (ppm)	C ₁₁ (ppm)	C ₁₄	C ₁₆ -C ₁₇
GBT(C ₈ H ₉ N ₄ S)	186.22	117.97, 120.63	125.42, 131.02	121.24, 152.35	167.02		
GPBT(C ₁₁ H ₁₅ N ₄ SPO ₃)	169.63	95.66, 97.00	123.49, 126.99	118.69, 127.99	138.24		64.17

Table 6: Selected IR bands (cm⁻¹) of GBT, GPBT and their metal complexes

S/N	L/Cplx	v(NH)	v(C-H)	v(C=C)	v(C=N)	v(C-N)	v(C-S)	v(P=O)	v(M-N)
1	GBT	3270-3394	3093	1635	1450	1103	760-632	-	-
2	Fe-GBT	3155	3090 w	1651 s	1396	1002	640	---	501
3	Co-GBT	3371	3093 w	1620 s	1380	1041	640	----	493
4	Ni-GBT	3371	3093	1643	1396	1118	640	---	493
5	Cu-GBT	3409	3091	1635	1388 s	1010	640	---	424
6	Zn-GBT	3201	3095	1620	1380	1026	717	----	555
7	GPBT	3417	3263	1635	1442	1172	748	1072	----
8	Fe-GPBT	3163		1666	1380	1064	vwb	1064	416
9	Co-GPBT	3394	3263 w	1651	1388	1072	vwb	1072	563
10	Ni-GPBT	3386	3263 w	1658	1380	1056	vwb	1056	578
11	Cu-GPBT	3348	3263 w	1658	1396	1064	763	1064	540
12	Zn-GPBT	3224	3263 w	1689	1342	1080	740	1080	555

vwb –very weak band.

Table 7 :UV-Visible electronic spectra and magnetic susceptibility of the GBT, GPBT and metal complexes.

Compounds	UV-Visible Spectra		Magnetic Moment μ_{eff} (B.M)	Probable Geometry
	Absorption (nm)	Transition		
C ₈ H ₉ N ₄ S	222, 260	$\pi \rightarrow \pi^*$, $n \rightarrow \pi^*$	-	
[Fe(C ₈ H ₉ N ₄ S) ₂]	320	CT	2.09	
[Co(C ₈ H ₉ N ₄ S) ₂]	530	4T _{1g} (F) \rightarrow 4T _{2g}	1.80	
[Ni(C ₈ H ₉ N ₄ S) ₂]	680, 720	3A _{2g} (F) \rightarrow 3T _{1g} (F) 3A _{2g} (F) \rightarrow 3T _{1g} (P)	3.14	
[Cu(C ₈ H ₉ N ₄ S) ₂]	780	3A _{2g} (F) \rightarrow 3T _{1g} (P),	2.10	
[Zn(C ₈ H ₉ N ₄ S) ₂]	730	3A _{2g} (F) \rightarrow 3T _{2g} (F),	0	
C ₁₁ H ₁₅ N ₄ SPO ₃	220,259	$\pi \rightarrow \pi^*$, $n \rightarrow \pi^*$	-	
[Fe(C ₁₁ H ₁₅ N ₄ SPO ₃) ₂]	340	CT	2.04	
[Co(C ₁₁ H ₁₅ N ₄ SPO ₃) ₂]	520	4A ₂ (F) \rightarrow 4T ₁ (P)	1.80	
[Ni(C ₁₁ H ₁₅ N ₄ SPO ₃) ₂]	630	3T ₁ (F) \rightarrow 3T ₁ (P)	3.09	
[Cu(C ₁₁ H ₁₅ N ₄ SPO ₃) ₂]	287	CT	2.12	
[Zn(C ₁₁ H ₁₅ N ₄ SPO ₃) ₂]	320	CT	0	

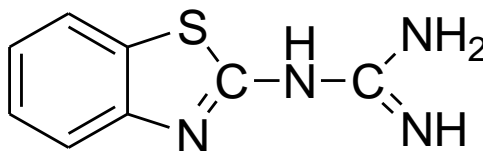


Figure 1: Probable Structure of guanidinobenzothiazole

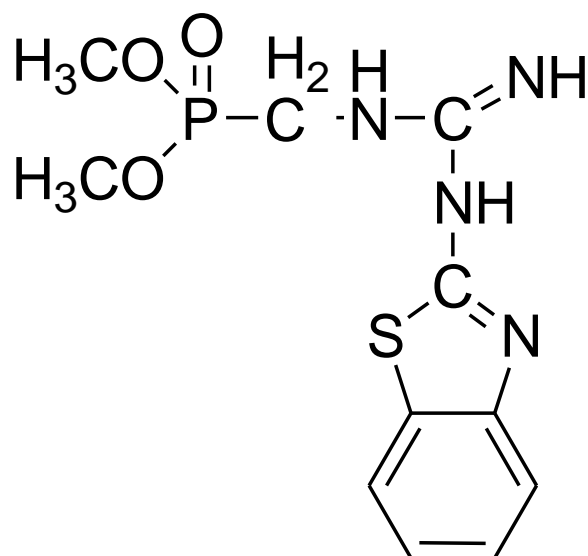
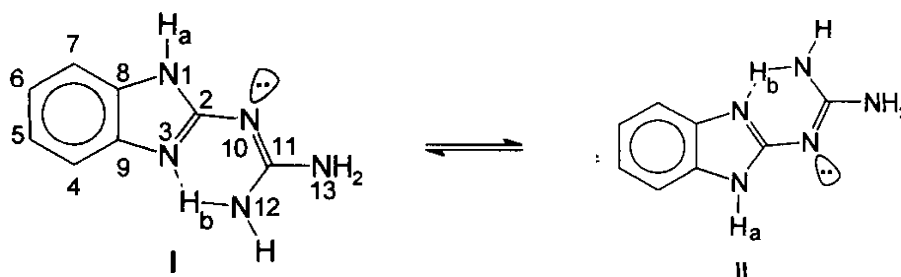


Figure 2: Probable Structure of guanidinophosphonatebenzothiazole

Chelating Properties and Proposed Structures for the Metal(II) –GBT and GPBT Complexes

The nitrogen atoms of guanidines play versatile roles towards coordination. The imidazolic N-3 and exocyclic N-10 of guanidines have been suggested as basic site for protonation, methylation, and coordination based on ^1H , ^{13}C , and ^{15}N NMR spectroscopy and X-ray diffraction (Andrade et al, 1997).



From the Infra-red, UV-Visible spectroscopic data, and magnetic susceptibility measurements, the following structures can be proposed for the metal(II) complexes of guanidinobenzothiazole, (GBT) and guanidinophosphonatebenzothiazole, (GPBT).

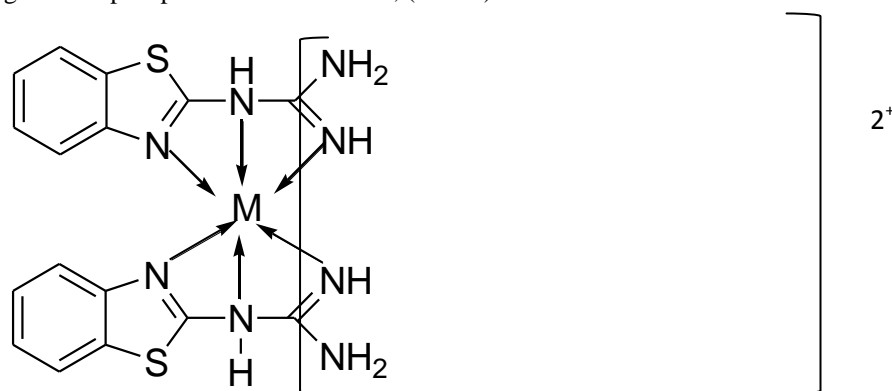


Figure 3 : Probable Structure of Metal (II) -guanidinobenzothiazole complex.
(Where M = Fe, Co, Ni, Cu and Zn)

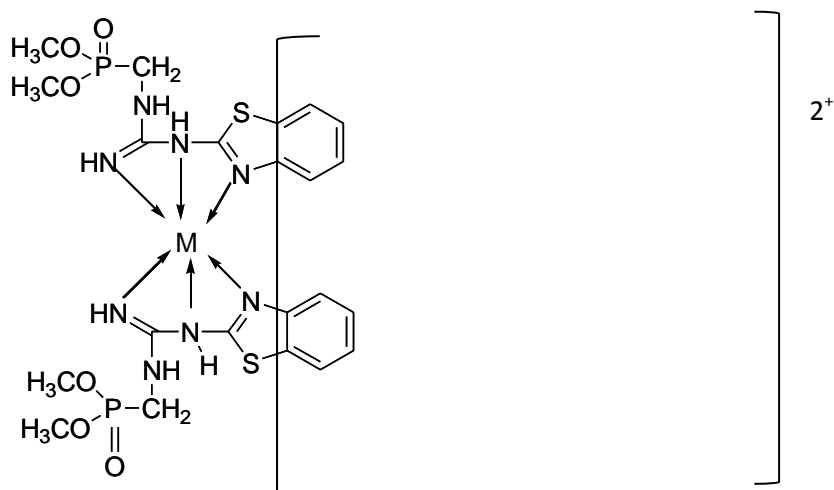


Figure 4: Probable Structure of Metal (II)-guanidinophosphonatebenzothiazole Where M = Fe, Co, Ni, Cu and Zn

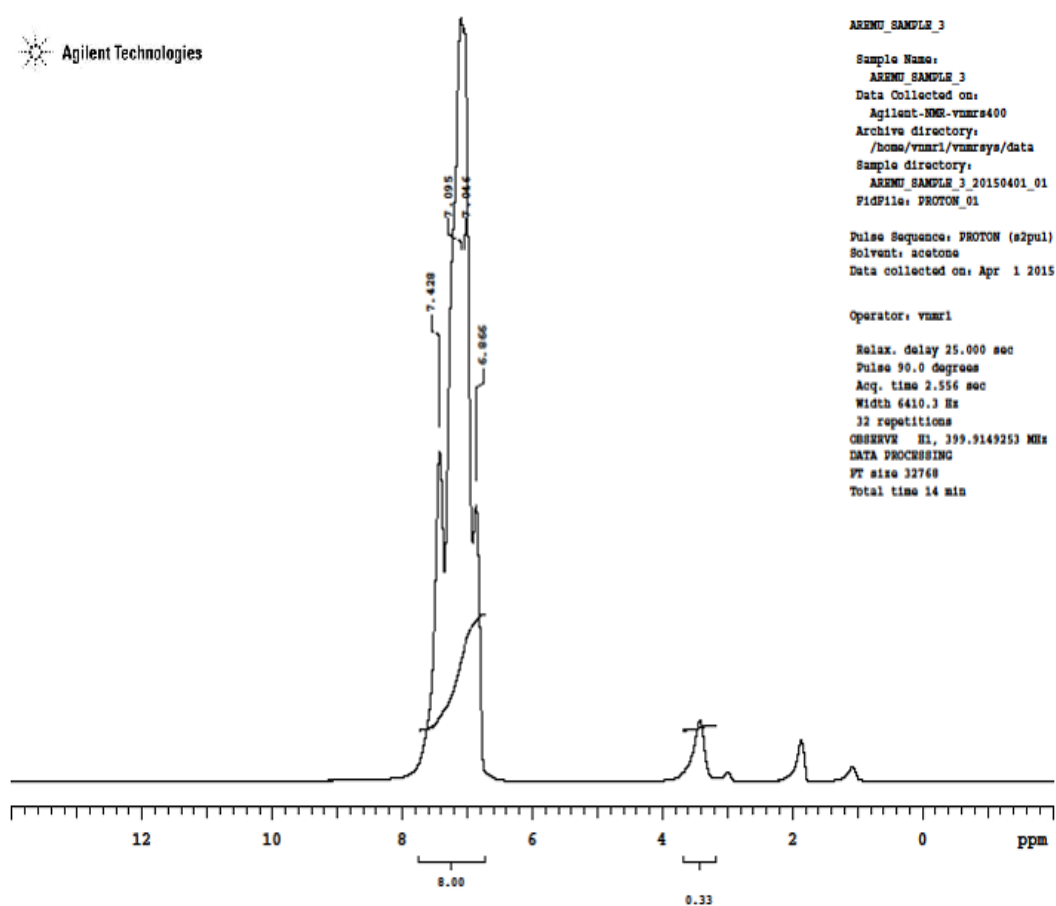


Figure 5: ^1H -NMR Spectrum of Guanidinobenzothiazole

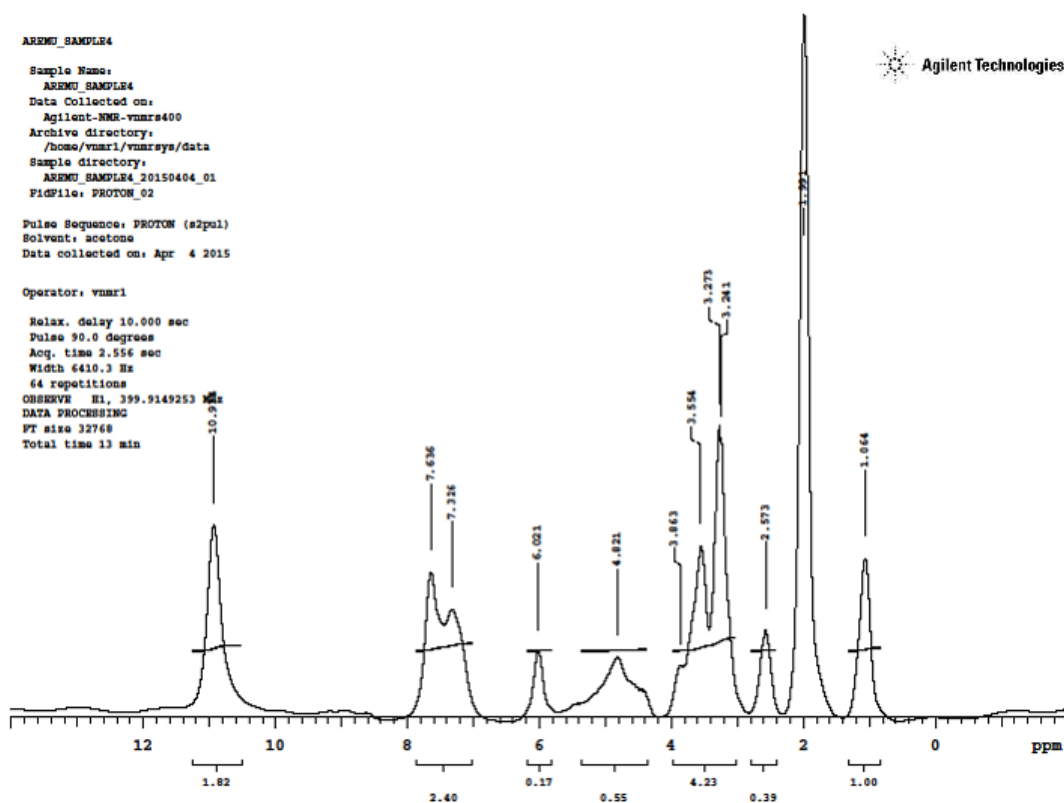


Figure 6: ¹H-NMR Spectrum of Guanidinophosphonatebenzothiazole

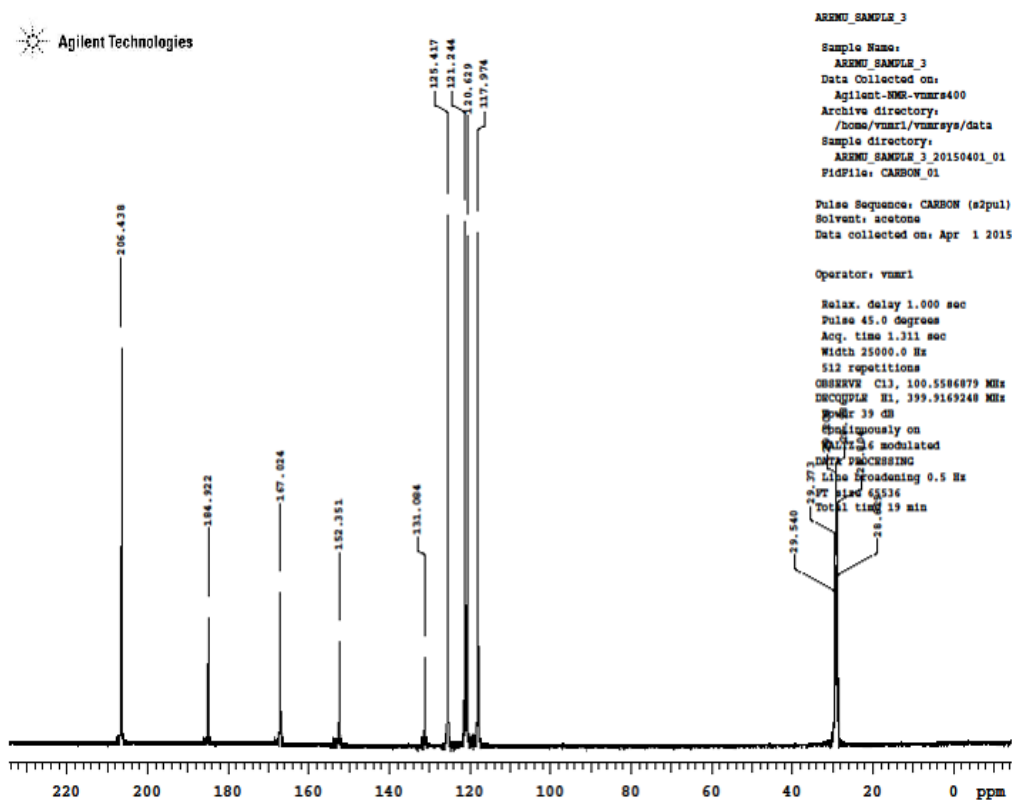


Figure 7: ¹³C-NMR Spectrum of Guanidinobenzothiazole

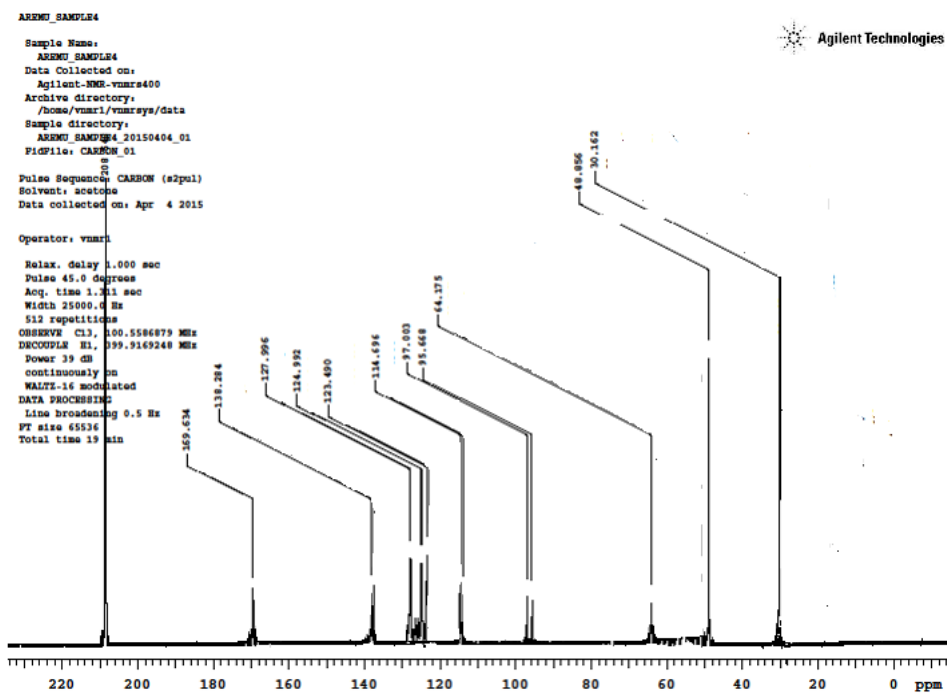


Figure 8: ¹³C-NMR Spectrum of guanidinophosphonatebenzothiazole

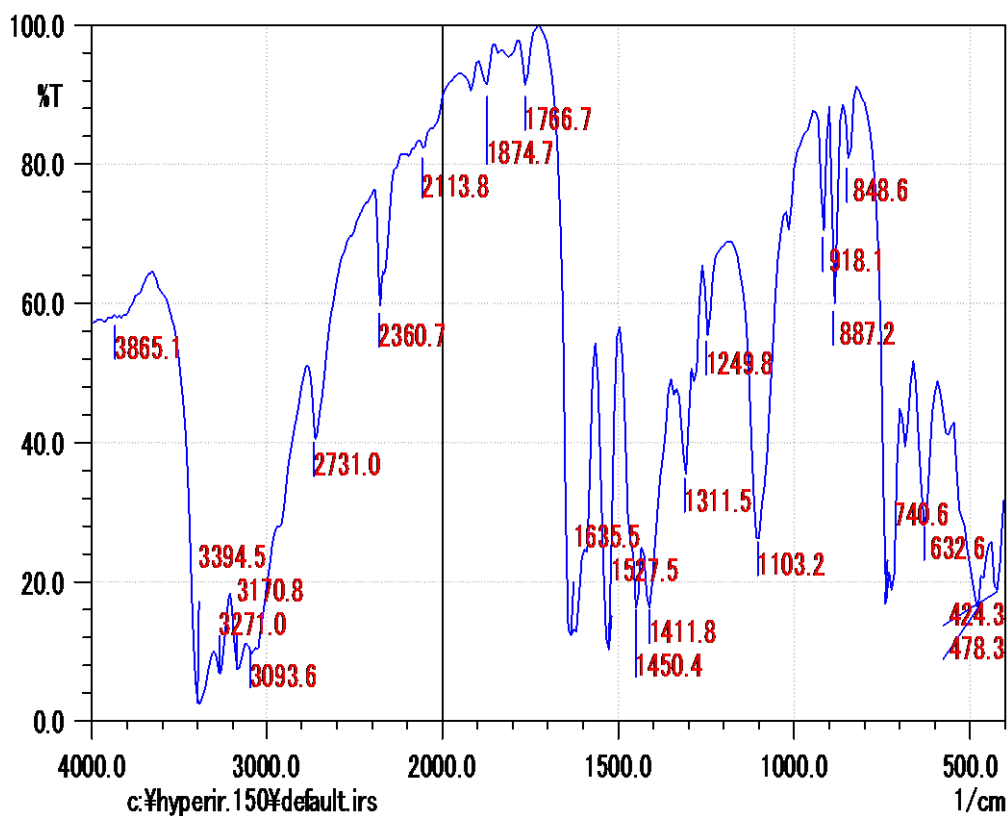


Figure 9: FT IR spectrum of guanidinobenzothiazole

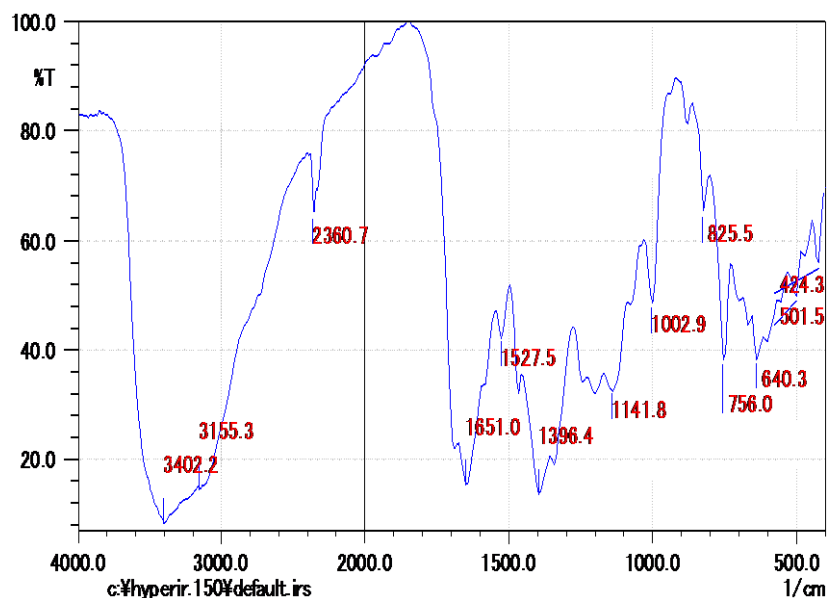


Figure 10: FT IR spectrum of Fe - guanidinobenzothiazole complex

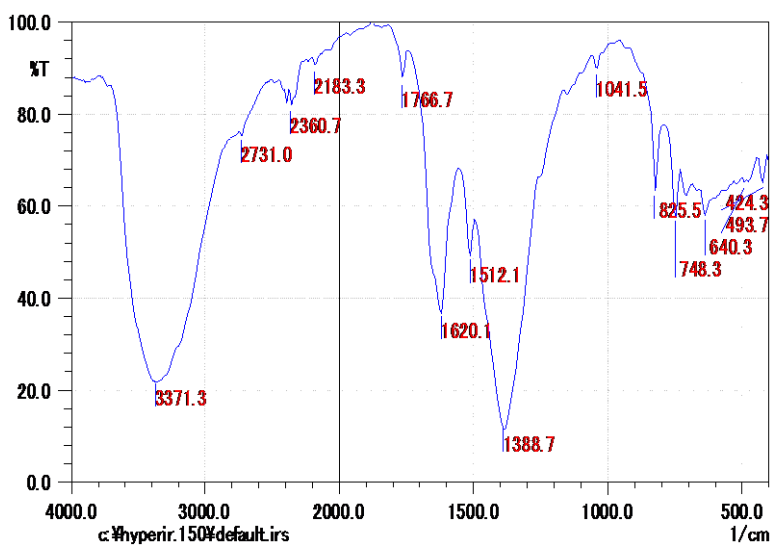


Figure 11: FT IR Spectrum of Co - guanidinobenzothiazole Complex

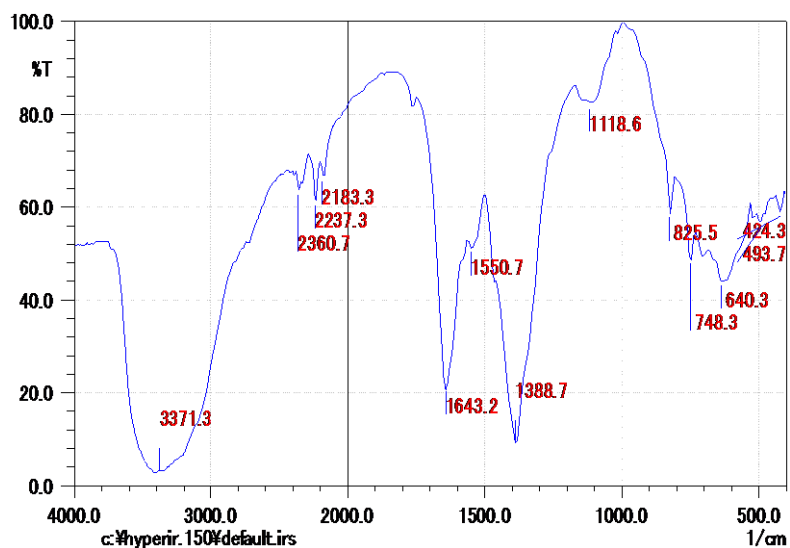


Figure 12: FT IR spectrum of Ni - guanidinobenzothiazole complex

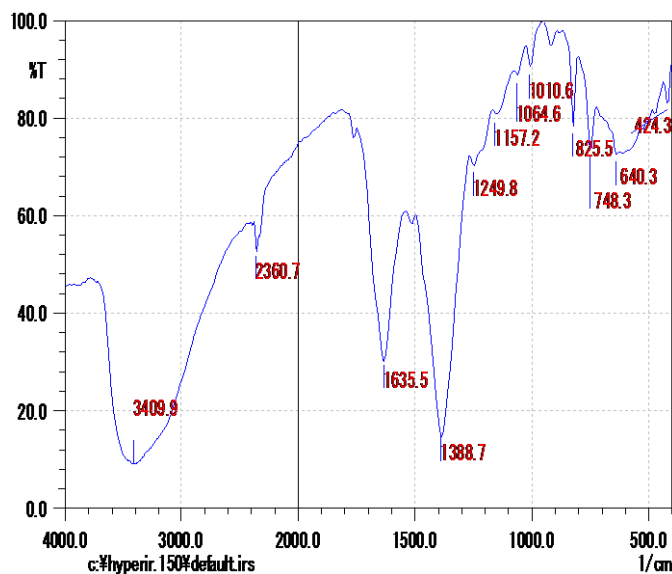


Figure 13: FT IR spectrum of Cu - guanidinobenzothiazole complex

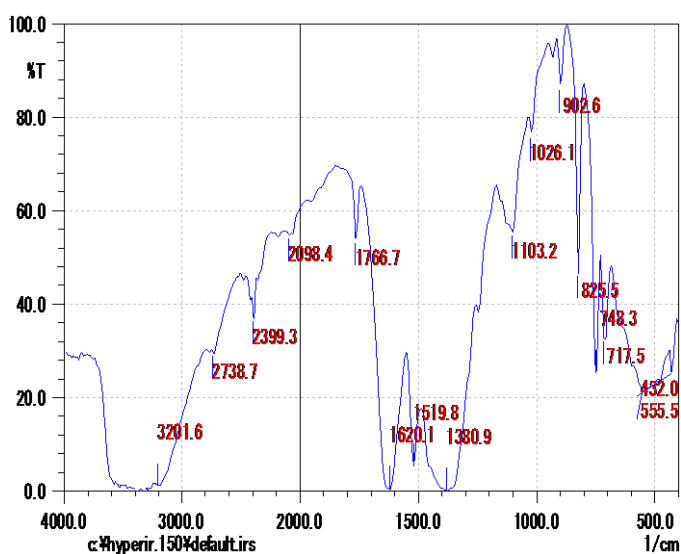


Figure 14: FT IR spectrum of Zn - guanidinobenzothiazole complex

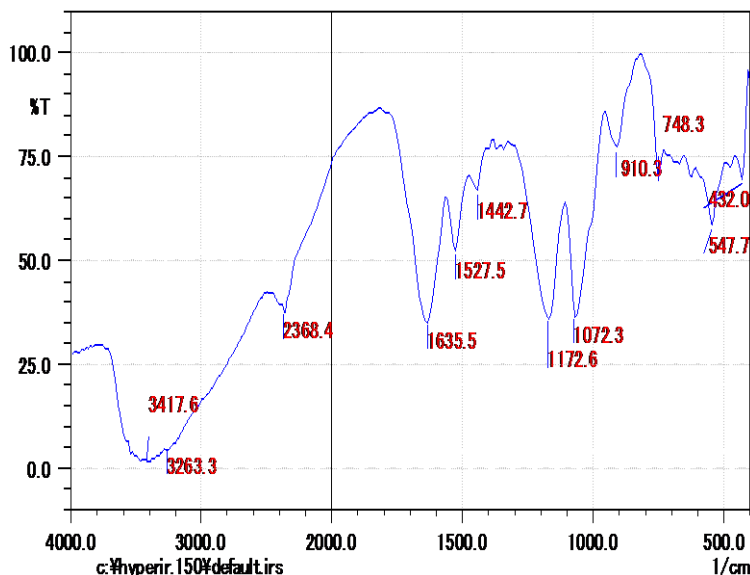


Figure 15: FT IR spectrum of guanidinophosphonatebenzothiazole

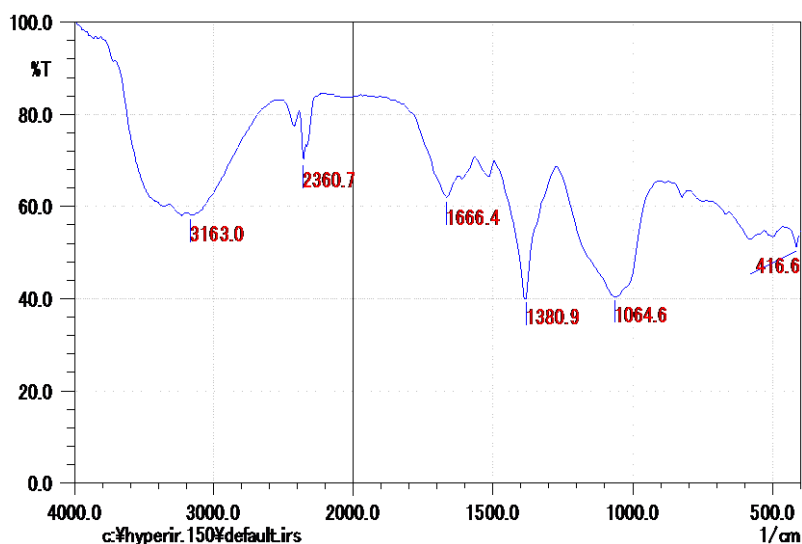


Figure 16: FT IR spectrum of Fe - guanidinophosphonatebenzothiazole complex

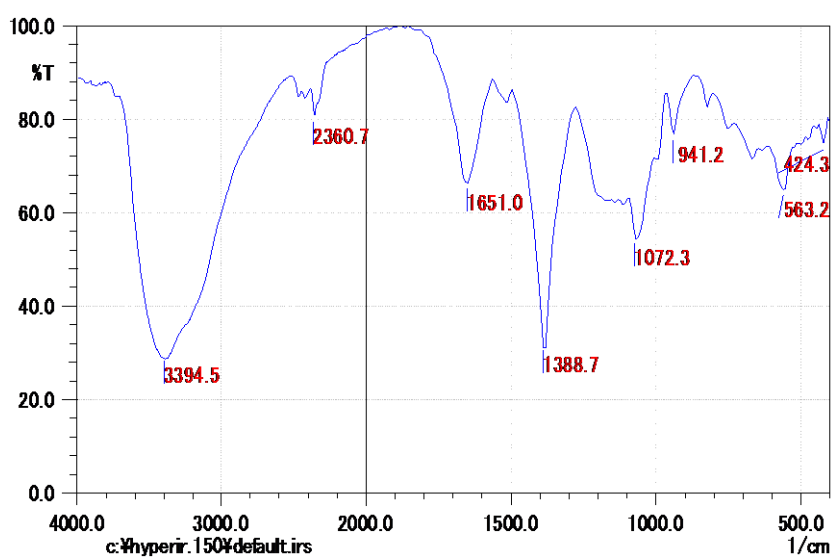


Figure 17: FT IR spectrum of Co - guanidinophosphonatebenzothiazole complex

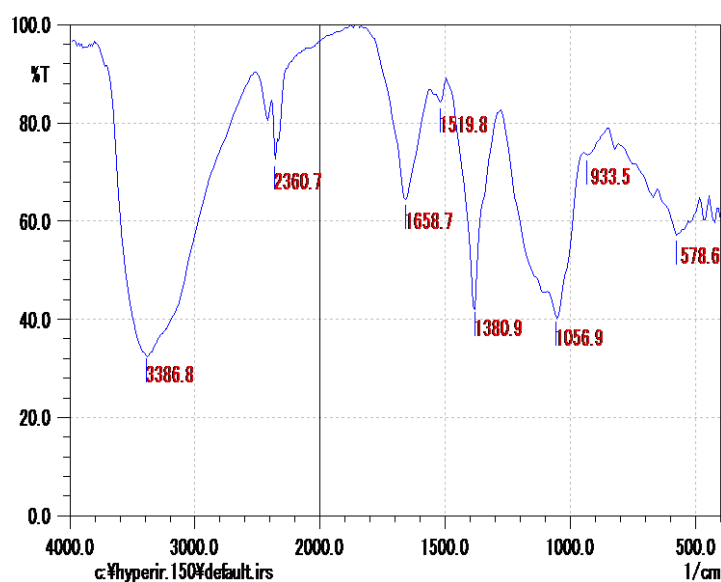


Figure 18: FT IR spectrum of Ni - guanidinophosphonatebenzothiazole complex

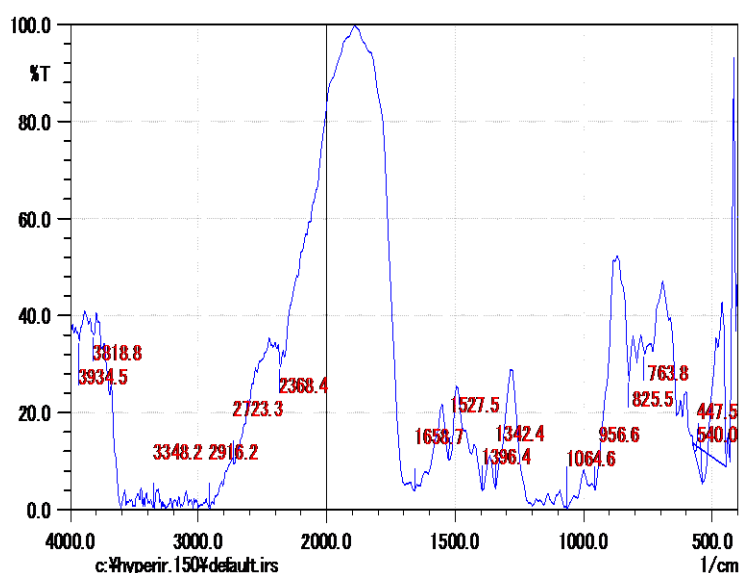


Figure 19: FT IR spectrum of Cu - guanidinophosphonatebenzothiazole complex

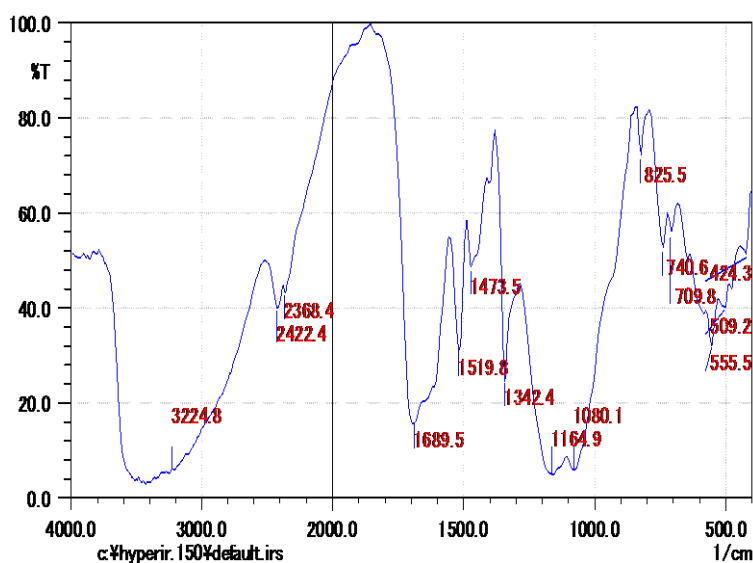


Figure 20: FT IR spectrum of Zn - guanidinophosphonatebenzothiazole complex

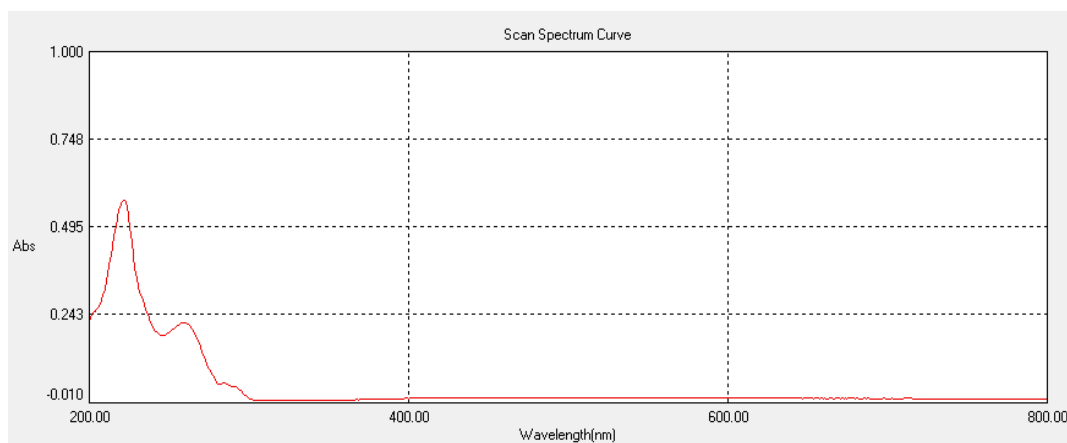


Figure 21: UV-Visible spectrum of guanidinobenzothiazole

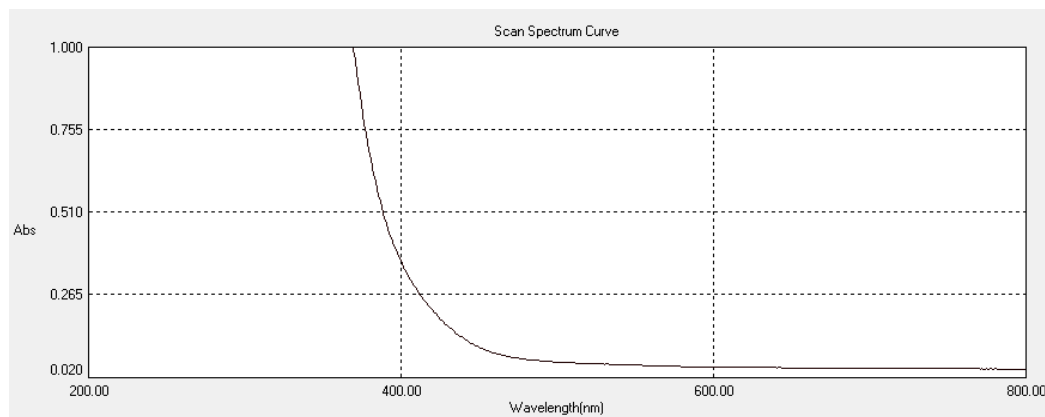


Figure 22: UV-Visible spectrum of Fe - guanidinobenzothiazole complex

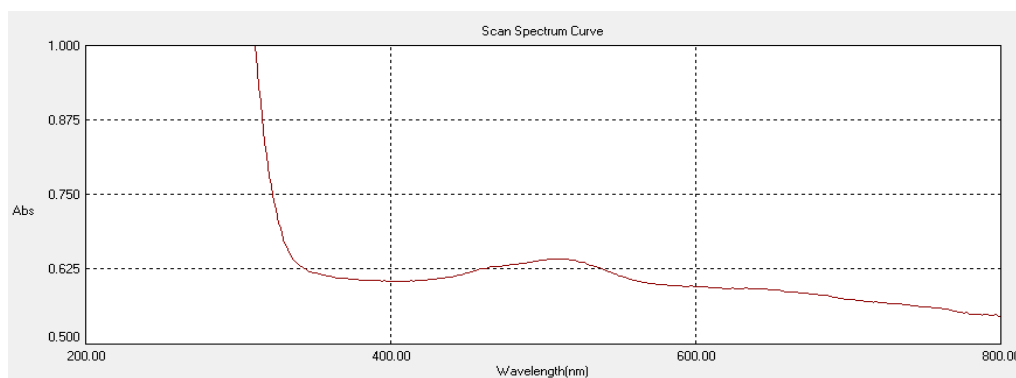


Figure 23: UV-Visible spectrum of Co - guanidinobenzothiazole complex

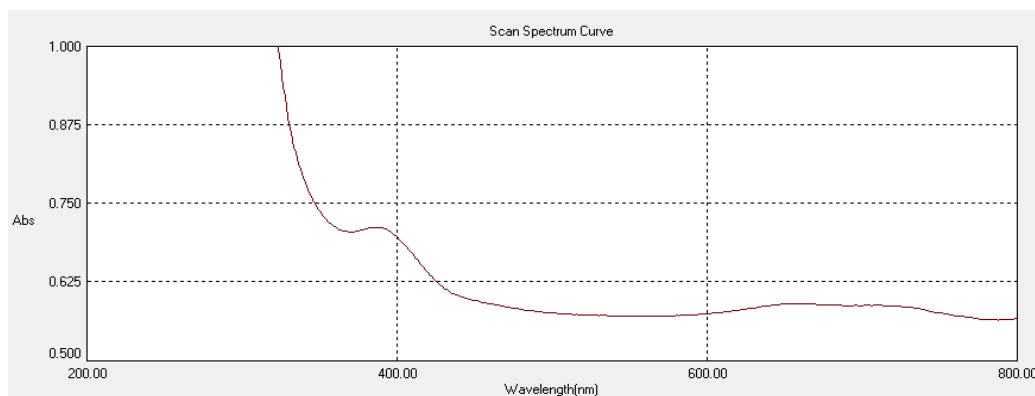


Figure 24: UV-Visible spectrum of Ni - guanidinobenzothiazole complex

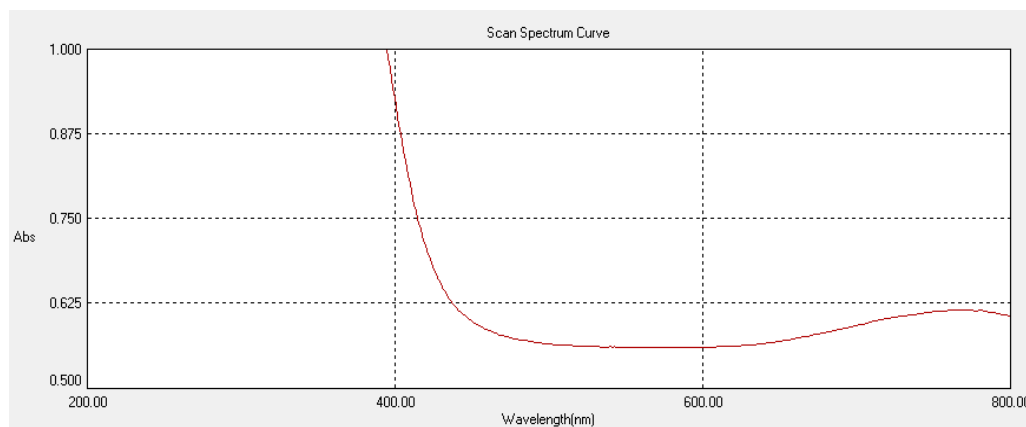


Figure 25: UV-Visible spectrum of Cu - guanidinobenzothiazole complex

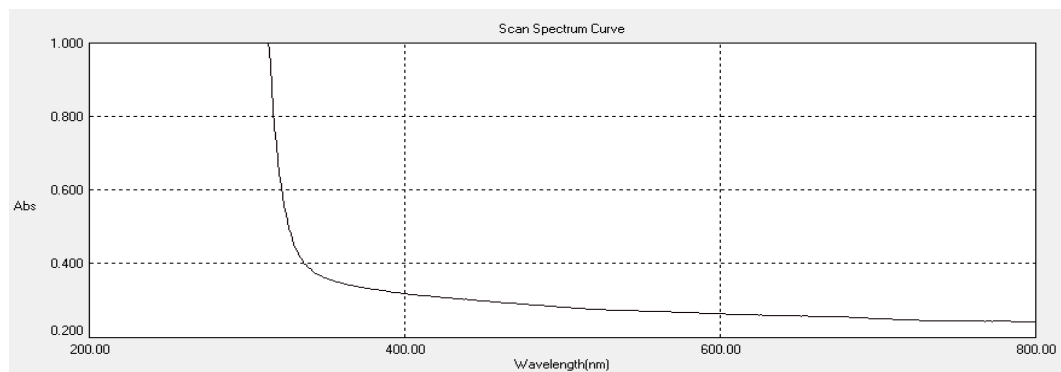


Figure 26:UV-Visible spectrum of Zn - guanidinobenzothiazole complex

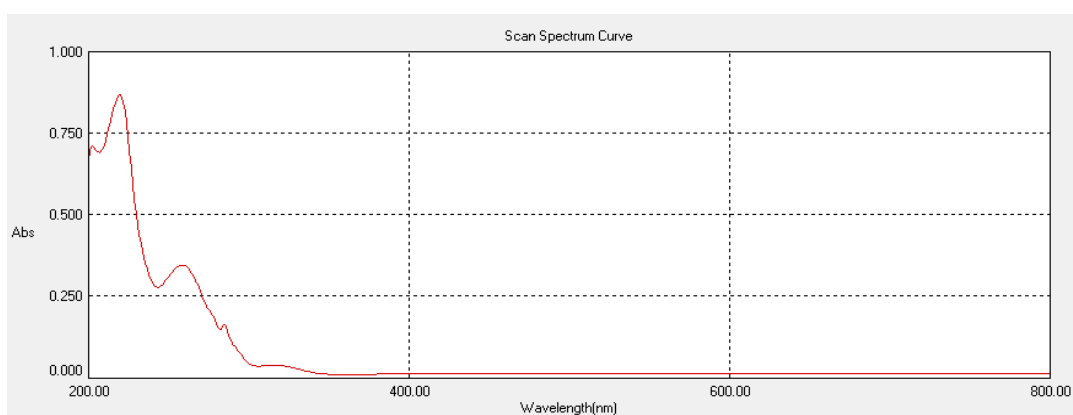


Figure 27:UV-Visible spectrum of guanidinophosphonatebenzothiazole

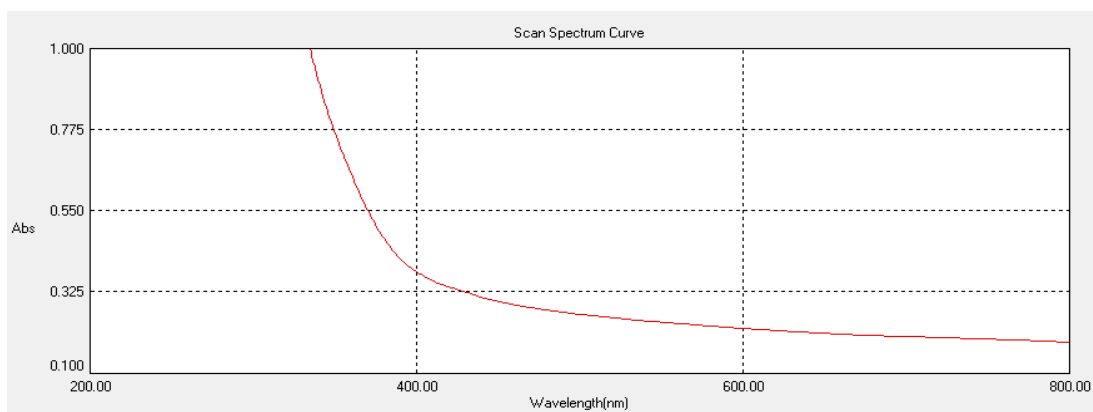


Figure 28:UV-Visible spectrum of Fe - guanidinophosphonatebenzothiazole complex

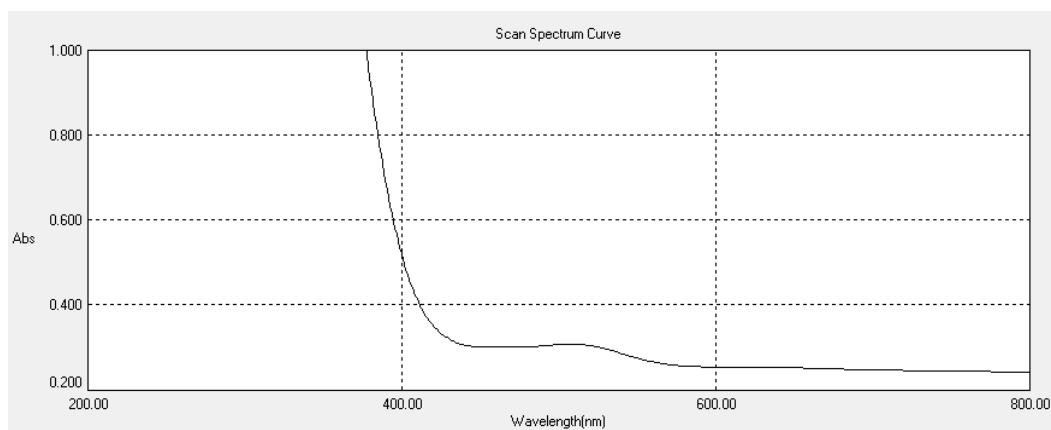


Figure 29: UV-Visible spectrum of Co - guanidinophosphonatebenzothiazole complex

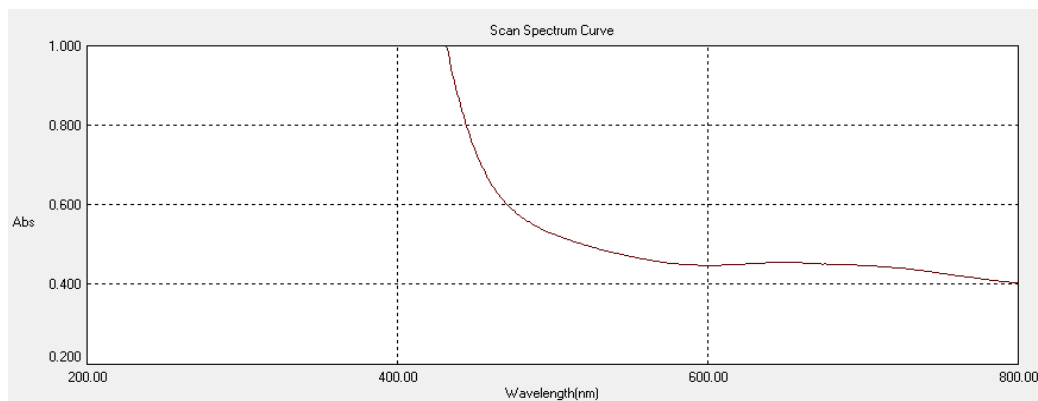


Figure 30: UV-Visible spectrum of Ni - guanidinophosphonatebenzothiazole complex.

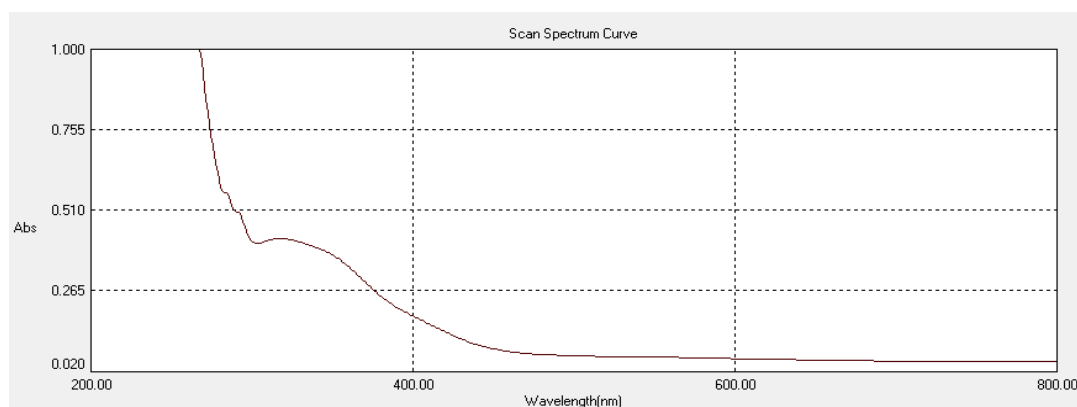


Figure 31: UV-Visible spectrum of Cu - guanidinophosphonatebenzothiazole complex.

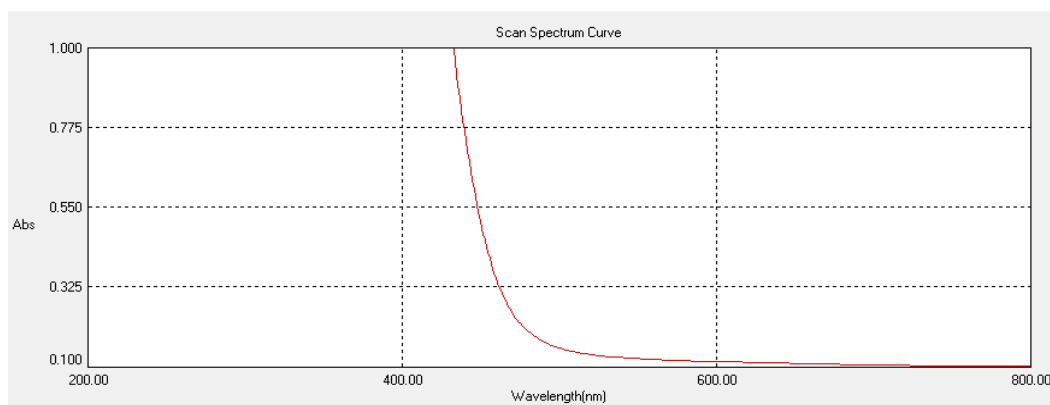


Figure 32: UV-Visible spectrum of Zn - guanidinophosphonatebenzothiazole complex

References

- [1]. Bradley, L. N. and Larry E. O. (2006). Concise Synthesis of Guanidine-Containing Heterocycles Using the Biginelli Reaction. *Journal of Organic Chemistry*, 71, 7706–7714
- [2]. Alan R. Katritzky*,[±] and Boris V. Rogovoy[§] (2005). Recent developments in guanylation agents, *Center for Heterocyclic Compounds, ARKIVOC*, (iv), 49-87.
- [3]. Yadav, P. S. and Devprakash, S. G. P. (2011). Benzothiazole: Different Methods of Synthesis and Diverse Biological Activities. *International Journal of Pharmaceutical Sciences and Drug Research*, 3, 01-071
- [4]. Malek, T. M.; Sayyed, M. H.; Reza, H.; Nourallah, H.; Seyed, S. S. and Mohsen, R. (2011). An efficient and simple synthesis of α -amino phosphonates as drug like molecules catalyzed by silica supported per chloric acid ($\text{HClO}_4\text{-SiO}_2$). *Arabian Journal of Chemistry*, 4, 481–485.
- [5]. Padmaja, M., Pragathi, J. and Kumari, C.G (2011). Synthesis, Spectral Characterization, Molecular Modeling and Biological Activity of First Row Transition Metal Complexes with Schiff Base Ligand Derived from Chromone-3-Carbaldehyde and o-Amino Benzoic Acid. *Journal of Chemical and Pharmaceutical Research*, 3, 602–613
- [6]. Malik, Sedlavora, E; Andriamanity, F; Sollei, C, (2006); Activity of Transition Metal Complexes of some Benzamides; *Journal of Pharmaceutical Sciences*, 75, 3-9.
- [7]. Rajkumar U. Pokalwar, Rajkumar V. Hangarge, Prakash V. Maskeb, and Murlidhar S. Shingare*, a (2006). Synthesis and antibacterial activities of α - hydroxyphosphonates and α acetyloxyphosphonates derived from 2-chloroquinoline-3- carbaldehyde . *General Papers ARKIVOC*. 196-204, 196.

- [8]. Daniel, H. O. D. and Isabel, R. I. A. (2011). Concise Synthesis of Asymmetrical N,N'Disubstituted Guanidines. *Tetrahedron Letters*, 5, 132.
- [9]. Krishnamurthy Ramadas and NatarajanSrinivasan (1995).An expedient synthesis of substituted guanidines.*Tetrahedron Letters*, Elsevier Science. 36, 2841-2844.
- [10]. Magsoodloua, M.T, Nourollah, Hazeria, S.M.Habibi-Khorassania, L.S, Mohammad,K.R; and Mojtaba, R.(2006); Diastereoselective synthesis of phosphonate esters by reaction between triphenylphosphite and acetylenic esters in the presence of NH-acid compounds, *ARKIVOC*, 13, 117-123.
- [11]. Anitha, C., Sumathi, I. S., Thamaraj, I.P. and Sheela, C. D. (2011). Synthesis, Characterization, and Biological Activity of Some Transition Metal Complexes Derived from Novel HydrazoneAzo Schiff Base Ligand. *International Journal of Inorganic Chemistry*, 201,1-8
- [13]. Bakir, S. R, Al-hamdani, A.A and Jarad. A. J. (2013). Synthesis and Characterization of Mixed Ligands of Dithizone and Schiff Base Complexes with Selected Metal Ions.*Journal for Pure Sciences*, 9, 82-94
- [14]. Srivastava, S. D. and Sen, J. P. (2008). Synthesis and Biological Evaluation of 2- Aminobenzothiazole Derivatives.*Indian Journal of Chemistry*. 47B, 1583-1586.
- [15]. Reddy, M. V. N., Kumar, B. S.,Balakrishna, A., Reddy, C. S., Nayak, S. K.and Reddy, C. D. (2007). One-pot Synthesis of Novel α -Amino Phosphonates using Tetramethyl guanidine as a Catalyst.*ARKIVOC*, 15, 246-254
- [17]. Andrade, N Ariza-Castolo, A.;andContreas,R;(1197); Versatile Behaviour of Guanidinobenzimidazole Nitrogen atoms toward protonation, Coordination and Methylation; *Heteroatom Chemistry*, 8, 397-410.
- [18]. Tarafder, M.T.H., Jin, K. T. Crouse, K.A., Ali, A.M., Yamin, B.M and Fun, H.-K., 2002. Coordination chemistry and bioactivity of Ni(II), Cu(II), Cd(II) and Zn(II) complexes containing bidentate Schiff bases derived from Sbenzylthiocarbamate and the X-ray crystal structure of bis[S-benzyl-N-(5-methyl-2-furylmethylene)dithiocarbamate]cadmium (II). *Polyhedron* 21, 2547-2554
- [20]. Lichty, J;Allen, S.M. Grillo, A.I, Archibald, J; Hubin, T.J. (2004), Synthesis and Characterisation of the Cobalt(III) Complexes of two pendant-Arm Cross bridged Cyclams; *Journal of Inorganic Chemistry*, 357, 615-618.
- [21]. Khatiwora, E., Mundhe, K., Deshpande, N.R. and Kashalkar. R.V. (2012). Anthelmintic activity of transition metal complexes of somebenzamidines. *Der PharmaChemica*, 4, 1264-1269
- [22]. Rao, C.N.R, Exkataraghavax, R; and Kasturi, T.R, (1964); Contribution to the Infrared Spectra of Organosulphur Compounds; *Canadian Journal of Chemistry*.vol. 42. 1964
- [24]. Zenobi MC¹, Luengo CV, Avena MJ, Rueda EH; (2008); *SpectrochimActa A MolBiomolSpectrosc.* 70(2):270-6.
- [25]. Onita, N., Şisu, I., Penescu, M., Purcarea, LV., Kurunczii, L. (2010). Synthesis, Characterization and Biological Activity of some α Aminophosphonates.*Farmacia*.58, 5531.
- [26]. Anderson, R; Bendell, D; and Groundwater, P; (2004); *Organic Spectroscopic analysis*; Royal Society of Chemistry, 22, 7-23

Aremu, J. A "Synthesis and Characterization of Guanidine derivatives of Benzothiazole and their Cobalt(II), Nickel(II), Zinc(II), Copper(II) and Iron(II) Complexes.." *IOSR Journal of Applied Chemistry (IOSR-JAC)* 11.1 (2018): 53-71.